Ester Manganiello[1], Marcus Herrmann[1], and Warner Marzocchi[1]

[1]Dipartimento di Scienze della Terra, dell'Ambiente e delle Risorse, Università degli

Studi di Napoli 'Federico II', Naples, Italy

Corresponding author: E. Manganiello, ester.manganiello@unina.it

Key Points:

- We compare the foreshock activity in southern California with the one predicted by the best-performing earthquake clustering model.
- We find that anomalous sequences with high number of foreshocks are mostly associated with a smaller mainshock magnitude.
- These anomalous sequences preferentially occur in zones of high heat flow, which are known for swarm-like seismicity.

Abstract

Foreshock analysis is expected to shed new light on the earthquake nucleation process and could potentially improve earthquake forecasting. Well-performing clustering models like the Epidemic-Type Aftershock Sequence (ETAS) model assume that foreshocks and general seismicity are generated by the same physical process, implying that foreshocks can be identified only in retrospect. However, several studies have recently found higher foreshock activity than predicted by the ETAS model. Here, we revisit the foreshock activity in southern California using different statistical methods and find anomalous foreshock sequences, i.e., those unexplained by ETAS, mostly for moderate mainshock magnitudes (magnitude 5.5 or smaller). The spatial distribution of these anomalies reveals that they preferentially occur in zones of high heat flow, which are known to host swarm-like seismicity. Outside these regions, the foreshocks generally behave as expected by ETAS. These findings may contribute to real-time detection of swarm-like activity and improve forecasting of large earthquakes.

Plain Language Summary

Many studies have observed that large earthquakes are preceded by smaller events, called foreshocks. If they have distinctive characteristics that make them recognizable in an ongoing sequence in real time, they can significantly improve the forecasting capability of large events. To investigate the nature of foreshocks, we compare real seismicity with the expectation of the most skilled earthquake clustering model, which assumes that foreshocks do not have any distinctive feature with respect to general seismicity. We find that discrepancies between the reality and the expectation mostly affect sequences characterized by a moderate mainshock magnitude. We show that those discrepancies tend to occur in zones of high heat flow, which are already known for the occurrence of swarm-like sequences. Outside these regions, the observed foreshocks activity

seems to be explained well by the clustering model. This finding urges the development of procedures that distinguish between swarms and classical earthquake sequences in real time, which will have a marked impact on the forecasting of large earthquakes.

1 Introduction

It is well known that many large earthquakes are preceded by smaller events (e.g., 1999 M7.6 Izmit, Turkey (Bouchon et al., 2011; Ellsworth & Bulut, 2018), 2009 M6.1 L'Aquila, Italy (Chiaraluce et al., 2011), 2011 M9.0 Tohoku, Japan (Kato et al., 2012), 2019 M7.1 Ridgecrest, USA (Meng & Fan, 2021)), which are (*a posteriori*) called foreshocks. The role of foreshocks in earthquake predictability can be epitomized by two still debated conceptual hypotheses about earthquake nucleation: the "pre-slip model" versus the "cascade model" (Ellsworth & Beroza, 1995; Gomberg, 2018). According to the former, foreshocks are triggered by an aseismic slip that anticipates the mainshock; in the latter model, foreshocks are like any other earthquake that trigger one another, with one of them eventually becoming exceedingly larger (the mainshock). For the 1999 Izmit sequence, Bouchon et al. (2011) and Ellsworth & Bulut (2018) found empirical contrasting evidence regarding the preferred model, only using data from a different number of seismic stations.

Notwithstanding the still active debate on these hypotheses, seismologists are not yet able to recognize foreshocks in real-time, tacitly implying that foreshocks are not different from the rest of the seismicity and indirectly supporting the cascade model hypothesis. This view is further supported by the fact that the current best performing short-term earthquake forecasting model (Taroni et al., 2018) – the Epidemic-Type Aftershock Sequences (ETAS) model – assumes that foreshocks, mainshocks, and aftershocks are undistinguishable and governed by the same process. ETAS belongs to the class of branching point process models known in the statistical literature as *Hawkes* or *self-exciting* point processes; in the ETAS model every earthquake can trigger other earthquakes according to established empirical relations and the magnitude of the triggered earthquake is independent from past seismicity.

Instead, if foreshocks are dominated by mechanisms other than earthquake triggering, as expected by the pre-slip hypothesis, they could be distinguished from general seismicity and potentially increase the probability for a larger earthquake to follow. For this reason, several studies recently investigated foreshock sequences of southern California and found that they deviate from expectations of the ETAS model. For example, Seif et al. (2019), Petrillo and Lippiello (2021), and Moutote et al. (2021) find, albeit at varying degrees, a higher foreshock activity in real seismicity than in synthetic catalogs simulated with ETAS. Therefore, the ETAS model appears to be unable to predict all the observed seismicity, which may suggest that foreshocks are distinct from general seismicity and governed by different mechanisms. These findings provide hope that foreshocks are distinguishable and potentially pave the way to a significantly improved earthquake predictability.

Here we reexamine foreshock activity in southern California and investigate the existence and main characteristics of foreshock sequences that cannot be explained by ETAS, i.e., anomalous foreshock sequences. We perform two different statistical analyses and consider the potential effect of subjective choices, such as the method to identify mainshocks and their foreshocks. To obtain clues about the main characteristics of possible anomalous foreshock sequences, we investigate different magnitude classes and analyze their spatial correlation with heat flow as a physical parameter. With our findings, we aim to contribute to the improvement of earthquake forecasting and the understanding of earthquake nucleation processes.

2 . Data and Methods

We use the relocated earthquake catalog for southern California catalog (Hauksson et al., 2012, see Data Availability Statement), selecting all earthquakes with M 2.5 from 1-1-1981 to 31-12-2019 except nuclear events (i.e., Nevada Test site) from the seismic catalog, totaling 47'574 events.

As there is no absolute and precise process to identify mainshocks, foreshocks, and aftershocks, the way of analyzing a seismic catalog and distinguishing these events is unavoidably subjective (Molchan & Dmitrieva, 1992; Zaliapin et al., 2008). To mitigate this subjective choice, we analyze the catalog using two quite different techniques: the Nearest-Neighbor (NN) clustering analysis proposed by Baiesi and Paczuski (2004) and elaborated by Zaliapin et al. (2008), and the spatiotemporal windows (STW) method.

The NN method expands the analysis of Baiesi and Paczuski (2004) in a space-time-magnitude domain based on the *nearest-neighbor distance* $_{ij}$, i.e., the minimal distance among event j and all earlier events i in the catalog. The event i with the shortest NN distance to event j is called nearest neighbor, or parent, event. By assigning a parent event to each event j, all events are associated with another. To identify individual families, i.e. sequences, or single events, we use the same threshold $_0 = 10^{-5}$ as Zaliapin et al. (2008), which effectively removes event associations with too large $_{ij}$. For each sequence, we refer to the event with the largest magnitude as the mainshock and all associated events that occur before it as its foreshocks. We only consider sequences with foreshocks and ignore those that have no foreshocks.

For the STW method, we initially consider all events with a magnitude M 4 as possible mainshocks. Then, we exclude events that are (i) preceded by a larger event within a spatiotemporal window of 10 km and 3 days before; (ii) preceded by an event with $M > 5$ within a window of 100 km and 180 days before; and (iii) not preceded by at least one event within a window of 10 km and 3 days. For the remaining mainshocks, all events within a window of 10 km and 3 days before each selected mainshock are considered foreshocks. The choice of the spatiotemporal windows was originally inspired by Felzer and Brodsky (2006).

To simulate synthetic catalogs, we use the ETAS model of K. Felzer (see Felzer et al., 2002, and Data Availability Statement) with parameters given by Hardebeck

et al. (2008, see supporting information Text S1 and Table S1). Using an available ETAS model reduces potential influences from subjective parameter choices on the analysis. We also verify the overall reliability of the ETAS model by comparing the number of events in the real catalog with the distribution of simulated events in the synthetic catalogs (see supporting information Text S2 and Figures S1and S2), finding that the ETAS model is consistent with the observation.

Once the mainshocks and their foreshocks have been identified in both the real and 1000 synthetic catalogs, we compare their foreshock statistics using two approaches named TEST1 and TEST2. In both tests, we examine if the actual observation is compatible with the synthetic catalogs.

TEST1 involves the average number of observed foreshocks per sequence, whereas TEST2, which has been inspired by the work of Seif et al. (2019), involves the frequency of observing a certain number of foreshocks per sequence. The two tests are described in detail below; they are somewhat related, but emphasize different aspects of the problem. We apply both tests to various mainshock magnitude classes $C_M = \{4.0 \leq m_M < 4.5,\ 4.5 \leq m_M < 5.0,\ 5.0 \leq m_M < 5.5,\ 5.5 \leq m_M < 6.0,\ m_M \geq 6.0\}$ and foreshock magnitude thresholds $T_F = \{m_F \geq 2.5,\ m_F \geq 3.0,\ m_F \geq 3.5,\ m_F \geq 4.0\}$; those choices are based on Seif et al. (2019), but we add the class $4.0 \leq m_M < 4.5$ to C_M. Although we report formal statistical test results, we underline that the significance of the tests is merely indicative since we do not formally account for applying the tests multiple times; the results are therefore meant to indicate possible patterns of (apparently) anomalous foreshock activity.

In TEST1, the null hypothesis under test $H_0^{(1)}$ is that the average number of foreshocks in the real catalog is not larger than the corresponding quantity in the synthetic catalogs.

For each mainshock magnitude class $c \in C_M$ and each foreshock magnitude threshold $t \in T_F$, we count the number of mainshocks $N_M^{(c,t)}$ and the number of foreshocks, $N_F^{(c,t)}$; $N_F^{(c,t)}$ is normalized by $N_M^{(c,t)}$ to obtain a single value $\widehat{N}_{\mathrm{F}}^{\mathrm{real}}$ for the real catalog. We calculate the same quantity in each i^{th} synthetic catalog, $\widehat{N}_{\mathrm{F}}^{\mathrm{ETAS}_i}$ and build its empirical cumulative distribution function (eCDF); if the observed $\widehat{N}_{\mathrm{F}}^{\mathrm{real}}$ is above the 99^{th} percentile of the eCDF, we reject the null hypothesis $H_0^{(1)}$ at a significance level of 0.01.

In TEST2, the null hypothesis under test $H_0^{(2)}$ is that for each number of foreshocks, N_{F}, the frequency of observed cases is not larger than the frequency observed in synthetic catalogs. For each mainshock magnitude class $c \in C_M$ and each foreshock magnitude threshold $t \in T_F$, we count the number of mainshocks that have a certain N_{F} (i.e., 1, 2, 3, etc.) and normalize it by the number of mainshocks in class c, $N_M^{(c,t)}$, that have foreshocks. In this way, we obtain the probability mass function (PMF) for the real catalog as a function of N_F. Then, we apply the same procedure to each synthetic catalog. For the whole

set of synthetic catalogs, we calculate the 99$^{\text{th}}$ percentile of the PMF values for each N_{F}. Finally, we reject the null hypothesis $H_0^{(2)}$ at a significance level of 0.01 if the PMF value of the real catalog is larger than this 99$^{\text{th}}$ percentile (i.e., the cases for which the real catalog contains more foreshocks than expected by ETAS). In essence, TEST2 seeks anomalies for every single N_{F}, whereas TEST1 could be seen as a cumulative version of TEST2.

To further investigate the physical interpretation of possible anomalous foreshock sequences in the real catalog, we analyze their spatial distribution. Specifically, taking inspiration from the previous work of Zaliapin and Ben-Zion (2013), we create a map by interpolating heat flow data (see Data Availability Statement) with a radial smoothing approach, which acknowledges areas without data; then we test if the distribution of heat flow values is significantly different at locations of normal and anomalous foreshock sequences. Specifically, we carry out two tests: the two-sample Kolmogorov-Smirnov test with the null hypothesis that the two distributions have the same parent distribution, and the Wilcoxon test with the null hypothesis that the distributions have the same median. In essence, the two-sample Kolmogorov-Smirnov test search for any kind of difference in the two distributions, whereas the Wilcoxon test is focused on testing if one distribution has higher values than the other.

3 . Results

3.1 Anomalous foreshocks

Figure 1 shows the results of TEST1 using NN to identify mainshocks and their foreshocks; the results using STW are reported in the supporting information (Figure S3). Each subplot shows the comparison of the cumulative distribution based on the synthetic catalogs with the observed value from the real catalog for each mainshock and foreshock magnitude class in C_M and T_F. A foreshock sequence is anomalous if the observed value (vertical black line) is above the 99$^{\text{th}}$ percentile of the distribution (vertical red line). As shown in Figure 1 and Figure S3, TEST1 results in a prevalence of anomalous foreshock sequences for smaller mainshock magnitudes. Of a total of 152 foreshock sequences, we found 61 (40%) to be anomalous; with the STW method we identified 143 foreshock sequences of which 34 (23%) are anomalous.

In Figure 2, we show the results of TEST2 for each mainshock and foreshock magnitude class in C_M and T_F using the NN method for foreshock and mainshock identification; the results using the STW method are reported in the supporting information (Figure S4). From Figure 2 we note that most of the PMF values of the real catalog are not anomalous (black triangles) because they are below the 99$^{\text{th}}$ percentile of the PMF values of synthetic catalogs (small grey dots); we find 21 of 152 (14%) foreshock sequences to be anomalous (red triangles), most of which are associated with smaller mainshock magnitudes. Figure 2 shows only eight red triangles (instead of 21) because some red triangles may represent several sequences or are outside the range of N_{F} used for the figure. The results using the STW method are similar: we find 10 of 143 (7%) foreshock

sequences to be anomalous.

For the sake of comparison, we also report the results obtained by Seif et al. (2019, blue circles) in Figure 2, who test a similar yet different null hypothesis than TEST2. Specifically, they treat all synthetic catalogs as one single compound catalog. Hence, the number of mainshocks that have a certain N_{F} is normalized by a total number of mainshocks regardless if they have foreshocks (as we do in TEST2) or no foreshocks. Note that in this way the PMF approaches increasingly lower values and moves further away from the real observation as the number of synthetic catalogs increases (i.e., lowering the detectable minimum frequency).

We repeated the above analyses at a 95% percentile significance level, which was originally used by Seif et al., (2019), and reported the results in the supporting information (Text S3 and Figure S5, S6, S7, and S8).

3.2 Correlation with the heat flow

In both tests, the most striking evidence for anomalies relates to the smaller mainshock magnitudes. This evidence may be related to two explanations: (i) the fact that those are more numerous, thus making the statistical test more powerful; or (ii) a physical reason that causes more foreshocks than assumed by the cascade model (triggering hypothesis). To discriminate between these two possibilities, we inspect the relation of the anomalies with the heat flow.

Figures 3a and 4a show the location of normal (empty circles) and anomalous (filled circles) foreshock sequences identified by TEST1 and TEST2, respectively, in a heat flow map. Figures 3b and 4b show the corresponding cumulative distributions of the interpolated heat flow observed at the location of normal (dashed curve) and anomalous (solid curve) foreshock sequences. In both cases, anomalous sequences tend to occur more frequently at locations of higher heat flow than normal sequences. The p-values of the two-sample Kolmogorov-Smirnov and Wilcoxon tests (see Figures 3b and 4b) are below 0.05, indicating that the two sample distributions come from different parent distributions with different means. This result corroborates the visual inspection of the maps: anomalous foreshock sequences preferentially occur in zones of high heat flow. Figures 3 and 4 are based on the NN method to identify mainshocks and their foreshocks; the results based on the STW method can be found in the supporting information (Figures S9 and S10) and confirm our findings. The results for using a significance level of 95% (in TEST1 and TEST2) are also shown in the supporting information for both NN method (Figures S11 and S12) and STW method (Figures S13 and S14).

Worthy of note, the heat flux data compared to the spatial coverage of the earthquake catalog are rather incomplete in the northern part of Mexico. For instance, several anomalous sequences occur in this area, but cannot be included in the heat flow analysis due to the lack of heat flow measurements. In addition, the available heat flow measurements in the northern part of Mexico are not consistent with the Geothermal map of North America (Blackwell & Richards,

2004), which indicates a generally high heat flow (> 100 $\mu W/m^2$) in this area along the San Andreas Fault.

4 . Discussion & Conclusion

We have found that foreshocks have the same characteristics of general seismicity as expected by ETAS, except in some cases. Our finding is in general agreement with previous studies of foreshock activity, all of which found (with some important differences not discussed here) higher foreshock activity than expected (Chen & Shearer, 2016; Moutote et al., 2021; Petrillo & Lippiello, 2021; Seif et al., 2019). However, our results additionally show—independently from the two tests and the two procedures to identify mainshocks and their foreshocks—that foreshock anomalies are associated with small mainshock magnitudes. The correlation with heat flow also indicates that these anomalies are preferentially (and statistically significant) located in zones of high heat flow. The combination of these two findings suggests that anomalous sequences behave more like seismic swarms. In fact, independent studies (e.g., Chen & Shearer, 2016; Ross et al., 2021; Zaliapin & Ben-Zion, 2013) have shown that swarm-like activity is common in those areas where we have found anomalous foreshock sequences.

The foreshock sequences that are preferentially located in zones of low-to-moderate heat flow are satisfactorily described by the ETAS model. The occurrence of both swarm-like and ETAS-like sequences implies that current clustering models used for forecasting large earthquakes may not be always appropriate. This facet raises an urgent need to find (quasi-)real-time methods to discriminate swarms from ETAS-like sequences. Such a method could lead to significant improvements in earthquake forecasting, for example in a swarm-like sequence with a markedly reduced forecast probability for a large earthquake. An interesting attempt in this direction has been made by Zaliapin and Ben-Zion (2013), who found that swarm-like sequences have a different topologic tree (i.e., internal clustering) structure that connect independent and triggered earthquakes. Unfortunately, this method can currently only be used retrospectively, limiting its applicability in earthquake forecasting. However, we envision other possible parameterizations of the topologic tree structure that may facilitate its use in a forecasting perspective.

Acknowledgments

This project has received funding from the European Union's Horizon 2020 research and innovation program under Grant Agreement Number 821115, Real-Time Earthquake Risk Reduction for a Resilient Europe (RISE).

Open Research

The southern California catalog of Hauksson et al. (2012) was obtained from https://scedc.caltech.edu/data/alt-2011-dd-hauksson-yang-shearer.html, version "1981–2019" (last accessed April 2021). Heat flow data were obtained from the following sources: National Geothermal Data System (http://geothermal.smu.edu/static/DownloadFilesButtonPage.htm, last accessed May 2021),

in particular the data sets '*Aggregated Well Data*', '*Heat Flow Observation in Content Model Format*', '*SMU Heat Flow Database of Equilibrium Log Data and Geothermal Wells*'; '*SMU Heat Flow Database from BHT Data*'; and RE Data Explorer (https://www.re-explorer.org/re-data-explorer/download/rede-data, last accessed May 2021) for data from Mexico. The ETAS simulator of K. Felzer was obtained from https://pasadena.wr.usgs.gov/office/kfelzer/AftSimulator.html (last accessed January 2021).

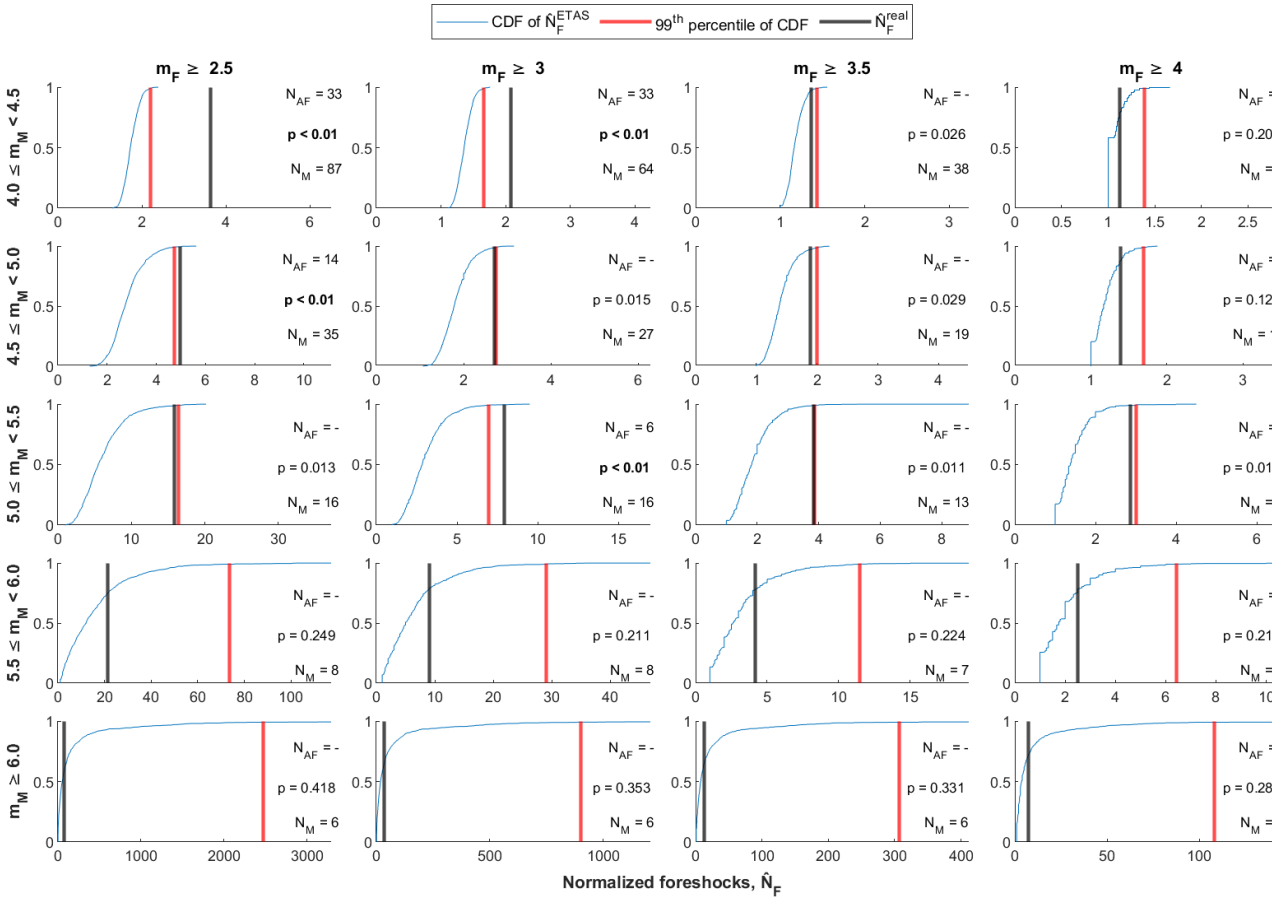

1. Results of TEST1 for various classes of the mainshock magnitude m_M (rows) and thresholds for the foreshock magnitude m_F (columns) in multiple subplots. Each subplot displays the number of normalized foreshocks for the real catalog (black vertical lines) and the empirical Cumulative Distribution Function (eCDF) with its 99$^{\text{th}}$ percentile (red vertical lines) for 1000 synthetic catalogs. Each subplot also reports the number of anomalous foreshock sequences, N_{AF}, the p-value for TEST1, and the number of mainshocks, N_M. The results are based on the NN method; supporting information Figure S3 shows results based on the STW method.

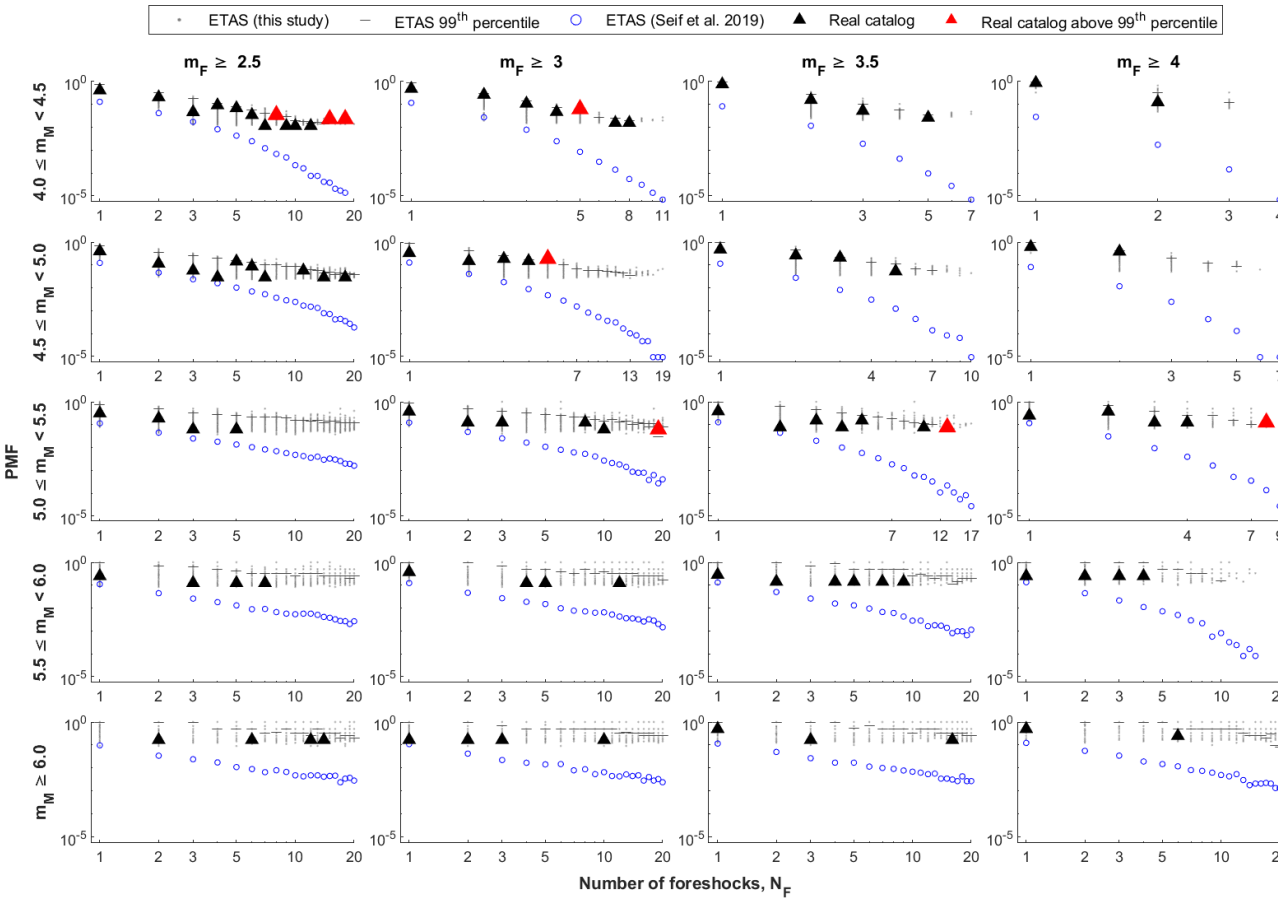

Figure 2. Results of TEST2 showing probability mass functions (PMF) of the number of foreshocks N_F for various classes of the mainshock magnitude m_M (rows) and thresholds for the foreshock magnitude m_F (columns). The PMFs are shown for the real catalog (black triangles), each synthetic catalog (small gray dots) and their 99th percentile (gray horizontal bars), and when considering all synthetic catalogs as a single compound catalog (blue open circles, reproducing Seif et al., 2019). Red triangles are above the 99th percentile of the PMF values for synthetic catalogs. The results are based on the NN method to identify mainshocks and their foreshocks; supporting information Figure S4 shows results based on the STW method.

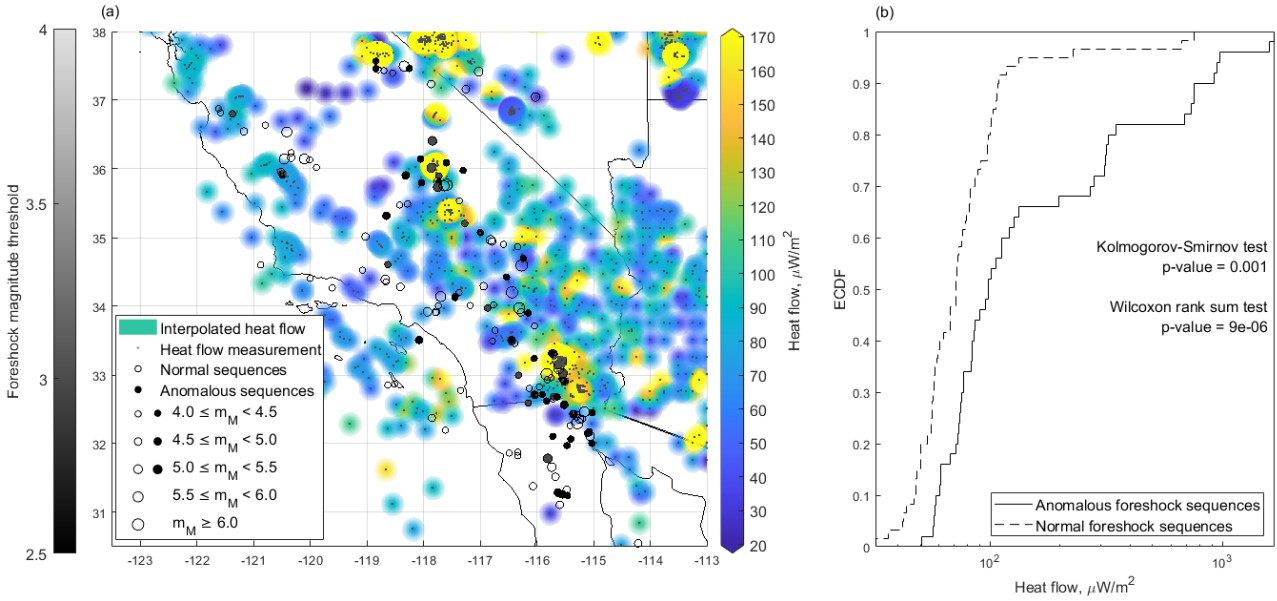

Figure 3. (a) Locations of normal foreshock sequences (empty circles) and anomalous foreshock sequences (filled circles) identified with TEST1 shown in a heat flow map. The size of the circles scales with the mainshock magnitude, m_M, (see legend) and their intensity with the foreshock magnitude, m_F, threshold (see color bar). The interpolated heat flow map is based on sampled heat flow measurements (small gray dots, see text in Data and Methods section); (b) CDF of heat flow values for normal (dashed curve) and anomalous foreshock sequences (solid curve). The results are based on the NN method; supporting information Figure S9 shows results based on the STW method.

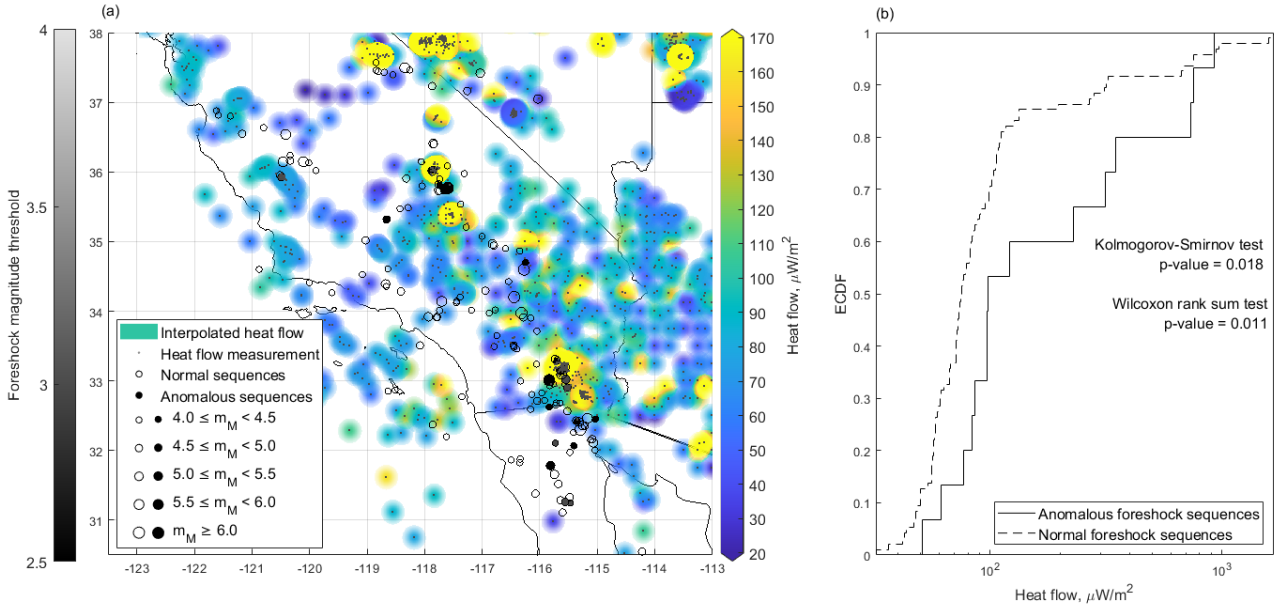

Figure 4. Like Figure 3 but showing anomalous foreshock sequences detected with TEST2. Supporting information Figure S10 shows results based on the STW method.

References

Baiesi, M., & Paczuski M. (2004). Scale-free networks of earthquakes and aftershocks. *Physical Review E*, *69*, 066106. https://doi.org/10.1103/PhysRevE.69.066106.

Blackwell, D. D., & Richards, M. (2004). Geothermal Map of North America, AAPG Map, scale 1:6,500,000, Product Code 423

Bouchon, M., Karabulut, H., Aktar, M., Özalaybey, S., Schmittbuhl, J., & Bouin, M. P. (2011). Extended Nucleation of the 1999 Mw 7.6 Izmit Earthquake. *Science*, *331*(6019), 877–880. doi: 10.1126/science.1197341

Chen, X. & Shearer, P. M. (2016). Analysis of Foreshock Sequences in California and Implications for Earthquake Triggering. *Pure Applied Geophysical*, *173*(1), 133–152. doi: 10.1007/s00024-015-1103-0

Chiaraluce, L., Chiarabba, C., De Gori, P., Di Stefano, R., Improta, L., Piccinini, D., Schlagenhauf, A., Traversa, P., Valoroso, L., & Voisin, C. (2011). The 2009 L'Aquila (central Italy) seismic sequence. *Bollettino di Geofisica Teorica ed Applicata*, *52*(3), 367-387. doi: 10.4430/bgta0019

Ellsworth, W. L., & Beroza, G. C. (1995). Seismic Evidence for an Earthquake Nucleation Phase. *Science*, *268*, 851-855. doi: 10.1126/science.268.5212.851

Ellsworth, W. L., & Bulut, F. (2018). Nucleation of the 1999 Izmit earthquake by a triggered cascade of foreshocks. *Nature Geoscience*, *11*(7), 531–535. https://doi.org/10.1038/s41561-018-0145-1

Felzer, K. R., & Brodsky, E. E. (2006). Decay of aftershock density with distance indicates triggering by dynamic stress. *Nature*, *441*, 735–738. https://doi.org/10.1038/nature04799

Felzer, K. R., Becker, T. W., Abercrombie, R. E., Ekström, G., & Rice, J. R. (2002). Triggering of the 1999 M_w 7.1 Hector Mine earthquake by aftershocks of the 1992 M_w 7.3 Landers earthquake. *Journal of Geophysical Research*, *107*(B9), 2190. https://doi.org/10.1029/2001JB000911

Gomberg, J. (2018). Unsettled earthquake nucleation. *Nature Geoscience*, 11(7), 463–464. https://doi.org/10.1038/s41561-018-0149-x

Hardebeck, J. L., Felzer, K. R., & Michael, A. J. (2008). Improved tests reveal that the accelerating moment release hypothesis is statistically insignificant. *Journal of Geophysical Research*, *113*, 3B08310. doi: 10.1029/2007JB005410

Hauksson, E., Yang, W., & Shearer, P. M. (2012). Waveform relocated earthquake catalog for Southern California (1981 to June 2019). *Bulletin of the Seismological Society of America*, *102*(5), 2239–2244. doi:10.1785/0120120010

Kato, A., Obara, K., Igarashi, T., Tsuruoka, H., Nakagawa, S., & Hirata, N. (2012). Propagation of Slow Slip Leading Up to the 2011 Mw 9.0 Tohoku-Oki Earthquake. *Science*, *335*(6069), 705-708. doi: 10.1126/science.1215141

Meng, H., & Fan, W. (2021). Immediate foreshocks indicating cascading rupture developments for 527 M 0.9 to 5.4 Ridgecrest earthquakes. *Geophysical Research Letters*, *48*, e2021GL095704. doi: 10.1029/2021GL095704

Molchan, G. M., & Dmitrieva, O. E. (1992). Aftershock identification: methods and new approaches. *Geophysical Journal International*, *109*(3), 501–516. https://doi.org/10.1111/j.1365-246X.1992.tb00113.x.

Moutote, L., Marsan, D., Lengliné, O., & Duputel, Z. (2021). Rare occurrences of non-cascading foreshock activity in Southern California. *Geophysical Research Letters*, *48*, e2020GL091757. https://doi.org/10.1029/2020GL091757

Petrillo, G., & Lippiello, E. (2021). Testing of the foreshock hypothesis within an epidemic like description of seismicity. *Geophysical Journal International*, *225*, 1236–1257. https://doi.org/10.1093/gji/ggaa611

Ross, Z. E, Cochran, E. S., Trugman, D. T., & Smith, J. D. (2021). 3D fault architecture controls the dynamism of earthquake swarms. *Science*, *368*(6497), 1357-1361. https://doi.org/10.1126/science.abb0779

Seif, S., Zechar, J. D., Mignan, A., Nandan, S., & Wiemer, S. (2019). Foreshocks and Their Potential Deviation from General Seismicity. *Bulletin of the Seismological Society of America*, *109* (1), 1–18. https://doi.org/10.1785/0120170188

Taroni, M., Marzocchi, W., Schorlemmer, D., Werner, M. J., Wiemer, S., Zechar, J. D., Heiniger, L., & Euchner, F. (2018). Prospective CSEP Evaluation of 1-Day, 3-Month, and 5-Yr Earthquake Forecasts for Italy. *Seismological Research Letters*, *89*, 1251-1261. doi: 10.1785/0220180031

Zaliapin, I., & Ben-Zion, I. (2013). Earthquake clusters in southern California I: Identification and stability. *Journal of Geophysical Research: Solid Earth*, *118*, 2847-2864. https://doi.org/10.1002/jgrb.50179

Zaliapin, I., & Ben-Zion, I. (2013). Earthquake clusters in southern California II: Classification and relation to physical properties of the crust. *Journal of Geophysical Research: Solid Earth*, *118*, 2865-2877. http://doi.org/10.1002/jgrb.50178

Zaliapin, I., Gabrielov, A., Keilis-Borok, V., & Wong, H. (2008). Clustering Analysis of Seismicity and Aftershock Identification. *Physical Review Letters*, *101*, 018501. https://doi.org/10.1103/PhysRevLett.101.018501